Theoretical study of electronic, magnetic, and structural properties of α-Fe_2O_3 (hematite)

M. Catti and G. Valerio
Dipartimento di Chimica Fisica ed Elettrochimica, Università di Milano, via Golgi 19, 20133 Milano, Italy

R. Dovesi
Dipartimento di Chimica Inorganica, Fisica e dei Materiali, Università di Torino, via Giuria 5, 10125 Torino, Italy
(Received 3 November 1994)

Antiferromagnetic rhombohedral α-Fe_2O_3 has been studied by calculations of the ground-state spin-polarized wave function and total energy, using the *ab initio* periodic unrestricted Hartree-Fock approach. All-electron basis sets of contracted Gaussian-type functions are employed to represent the O and Fe atoms (18 and 27 orbitals, respectively); Fe is alternatively described by a large-core pseudopotential plus 18 valence-shell orbitals. Computations have been performed for both the antiferromagnetic (AF) and ferromagnetic (FM) structures; the correct relative stability is reproduced, with $\Delta E(\text{AF-FM}) = -0.0027$ hartree per formula unit (including a correction for correlation energy). The dependence of ΔE(AF-FM) on variations of the Fe-O bond lengths and Fe-O-Fe' angles involved in superexchange is analyzed, finding that for some configurations the FM structure becomes more stable than the AF one. The athermal equation of state, equilibrium crystal structure, elastic bulk modulus, and binding energy have been computed and compared to experimental quantities. An analysis of the density of electronic states show that the band gap is of *p-d* rather than *d-d* type, confirming the charge-transfer-insulator nature of hematite as inferred from photoelectron spectra. The overall shape of the valence band is also fully consistent with spectroscopic results. Mulliken electron population data indicate a charge back transfer of $0.29|e|$ from O^{2-} to the *d* shell of Fe^{3+}, causing a partial spin pairing with a magnetic moment of $4.7\mu_B$.

INTRODUCTION

The first-row transition-metal oxides are a class of materials with outstanding electronic and magnetic properties, which have been the object of intensive experimental and theoretical research for a long time.[1] Most work has concerned the compounds with 1:1 stoichiometry and NaCl-type crystal structure. In particular, these have been very recently investigated by *ab initio* periodic unrestricted-Hartree-Fock (UHF) methods,[2,3] which have proved to be suitable theoretical techniques for crystalline systems containing open-shell ions. Other calculations, based on the density-functional approach in conjunction with linearized augmented plane-waves (DFT-LAPW) schemes, have been reported.[4,5] Because of the high symmetry of the rocksalt structure, these oxides are relatively simple to study, but do not give information on more subtle questions such as the influence of bond angles on superexchange and magnetic properties. For this reason, and for the interest of considering oxides of transition metals in different oxidation states, the case of rhombohedral α-Fe_2O_3 (hematite) seems to be particularly attractive. Iron sesquioxide is an important antiferromagnetic material, and also occurs as a natural product of surface alteration of many iron-containing rock-forming minerals. Its study is framed into a theoretical investigation of corundum-type and spinel-type oxides, the first part of which concerned α alumina and magnesium aluminate.[6]

Hematite is isostructural with α-Al_2O_3 (space group $R\bar{3}c$, two and six formula units in the primitive rhom-

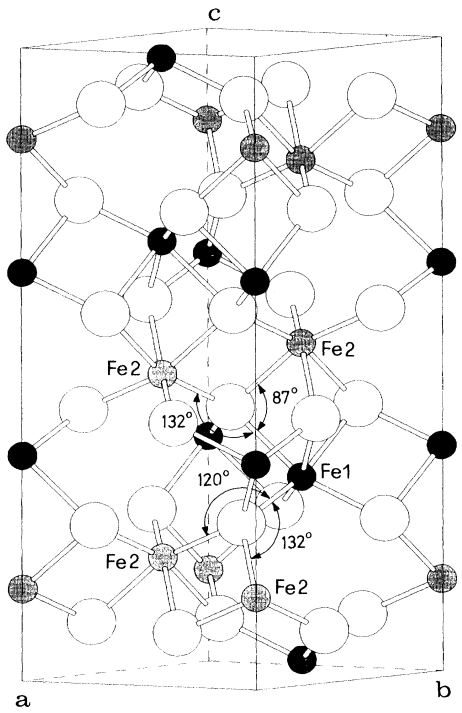

FIG. 1. View of the crystal structure of antiferromagnetic α-Fe_2O_3, with outline of the hexagonal unit cell. Black, gray, and open circles denote Fe1 (spin-up), Fe2 (spin-down), and O atoms, respectively. The angular superexchange interactions involving a particular Fe1 atoms, two neighboring oxygens, and the related Fe2 atoms are emphasized.

bohedral, and in the conventional hexagonal unit cells, respectively); its structure was refined from x-ray diffraction data at ambient conditions and also at high pressure.[7,8] Hexagonal close-packed (001) layers of O atoms are present, with Fe atoms filling $\frac{2}{3}$ of the octahedral holes in between (Fig. 1). The stable phase turns out to be antiferromagnetic (AF) below the Néel temperature $T_N=953$ K. In the corresponding magnetic structure (space group $R\bar{3}$), alternating (001) layers of spin-up (Fe1) and spin-down (Fe2) iron atoms are observed.[9] Out of the four Fe atoms in the primitive cell, two are independent (Fe1 and Fe2), and the other ones are centrosymmetrically related to them. Two different modifications of this antiferromagnetic structure are observed: below the Morin temperature ($T_M=250$ K) the Fe electron spins are aligned with the [001] hexagonal axis, while above T_M, they lie on the (001) planes.[10] A weak ferromagnetic moment is present at $T_M<T<T_N$, due to a slight canting of the spins.[11] A hypothetical ferromagnetic (FM) structure would correspond to space group $R\bar{3}c$ with four Fe1-type (spin-up) symmetry-related iron atoms in the primitive cell.

The electronic structure of α-Fe_2O_3 has been thoroughly investigated recently by photoelectron spectroscopy[12–14] and by inverse-photoemission techniques,[15] and the results have been interpreted as due to a charge-transfer insulator on the basis of configuration-interaction (CI) cluster calculations.[12] Some details of the interpretation of the density of electron energy states are still not completely understood, however. Other simpler cluster-type quantum-mechanical studies of the MS-$X\alpha$ type have been performed,[16,17] but no periodic calculations have appeared yet, to our knowledge.

The aim of the present study is to apply the UHF computational approach to the α-Fe_2O_3 crystalline system, which should be related to MnO (Ref. 3), because Fe^{3+} is a d^5 ion isoelectronic with Mn^{2+}. On the other hand, its more complex crystal structure is expected to introduce important differences both in the magnetic and in the electronic behavior with respect to MnO. Further, the structural changes of hematite with pressure and its athermal equation of state are investigated here, in order to compare them with the results found for isostructural corundum.

COMPUTATIONAL

Ab initio periodic LCAO (linear combination of atomic orbitals) Hartree-Fock methods, as implemented in the CRYSTAL92 code,[18] were used, adding the supplementary option for unrestricted treatment of the spin-dependent part of the wave function in open-shell systems.[19] The latter feature was essential to obtain spin-polarized eigenfunctions of the Fock Hamiltonian, taking into account the $1s^2 2s^2 2p^6 3s^2 3p^6 3d^5$ electronic configuration of isolated Fe^{3+} ions. The radial factors of atomic orbitals are

TABLE I. Exponents (bohr^{-2}) and contraction coefficients of the (individually normalized) Gaussian functions adopted for iron in the present study. $y[\pm z]$ stands for $y\times 10^{\pm z}$. Durand-Barthélat pseudopotential[21] (PP) and all-electron (AE) basis sets are reported.

Shell	Fe (PP)			Fe (AE)		
		Coefficients			Coefficients	
type	Exponents	s	p,d	Exponents	s	p,d
1s				3.154[+5]	2.270[−4]	
				4.569[+4]	1.900[−3]	
				9.677[+3]	1.110[−2]	
				2.521[+3]	5.010[−2]	
				7.597[+2]	1.705[−1]	
				2.630[+2]	3.692[−1]	
				1.028[+2]	4.033[−1]	
				4.297[+1]	1.434[−1]	
2sp				7.983[+2]	−5.200[−3]	8.500[−3]
				1.912[+2]	−6.800[−2]	6.080[−2]
				6.369[+1]	−1.314[−1]	2.114[−1]
				2.536[+1]	2.517[−1]	3.944[−1]
				1.073[+1]	6.433[−1]	3.980[−1]
				3.764	2.825[−1]	2.251[−1]
3sp				4.814[+1]	1.220[−2]	−2.150[−2]
				1.746[+1]	−2.278[−1]	−8.500[−2]
				6.997	−8.801[−1]	2.010[−1]
				3.079	9.755[−1]	1.302
4sp	1.486	3.365[−1]	1.0	1.314	1.0	1.0
	1.132	−5.327[−1]	1.0			
5sp	4.500[−1]	1.0	1.0	5.532[−1]	1.0	1.0
3d	4.081[+1]		2.574[−2]	3.048[+1]		5.830[−2]
	1.219[+1]		1.431[−1]	8.692		2.591[−1]
	4.126		3.535[−1]	3.101		5.162[−1]
	1.526		4.846[−1]	1.171		5.656[−1]
4d	5.117[−1]		1.0	4.298[−1]		1.000

expressed as linear combinations of Gaussian-type functions of the electron-nucleus distance. The O atom was represented on an all-electron basis by 18 atomic orbitals (Gaussian basis set of type[20] 8-411G*), according to the scheme previously[6] used for α-Al_2O_3; the Gaussian exponents and coefficients for the inner shells 1*s*, 2*sp*, and 3*sp* are therein reported. Iron was dealt with at an all-electron (AE) level, according to a 8-6-411G* contraction with two *d*-type (41G) shells. However, owing to limitations of the available computational resources, for some calculations it was necessary to devise a less expensive, slightly less satisfactory scheme. This was done by employing the Durand-Barthélat large-core pseudopotential,[21] supplemented by two *sp*-type (21G) and two *d*-type (41G) shells, to represent iron. The corresponding basis set, keeping the all-electron representation for oxygen, will be denoted as PP (pseudopotential), while the AE symbol is employed for the all-electron description of both the Fe and O atoms. Use of the PP scheme will be made in the study of the influence of structural changes on crystal properties. Further, assessing the overall performance of the PP with respect to AE basis set is useful, because in future studies of more complicated crystal structures, possibly containing second- or third-row transition elements, use of the less expensive PP scheme could be a necessary choice.

At first, the parameters of the AE and PP basis sets were optimized by minimizing the energy of the isolated Fe^{3+} ion. Then the exponents of the 5*sp* and 4*d* shells of Fe and those of the 4*sp* and 3*d* shells of O were refined by searching for the minimum total crystal energy of α-Fe_2O_3 at the experimental structural configuration. The optimized parameters of both basis sets of Fe are reported in Table I; the 4*sp* and 3*d* exponents obtained for oxygen are 0.210 and 0.35 $bohr^{-2}$ (AE), and 0.200 and 0.35 $bohr^{-2}$ (PP), respectively. Apart from the presence of a *d* orbital shell, and small differences for the two outer shells (3*sp* and 4*sp*) exponents, the O basis set is analogous to that used in studies of the rocksalt-type transition-metal oxides.[2,3] Also, the AE basis of iron interpolates well between those of Mn and Ni given in the same studies.

The level of numerical approximation in evaluating the Coulomb and exchange series appearing in the self-consistent-field (SCF) equations for periodic systems is controlled by five tolerances.[18] These are related to estimates of overlap or penetration for integrals of Gaussian functions on different centers, which define cutoff limits for series summation. The values used in the present calculations are 10^{-6}, 10^{-6}, 10^{-6}, 10^{-7}, and 10^{-13}, which correspond to severe computational conditions. The reciprocal space was sampled according to a regular sublattice defined by six points in the irreducible Brillouin zone.

EQUILIBRIUM AND HIGH-PRESSURE STRUCTURE

Although the AF configuration of hematite is the stable one at low temperature, as confirmed also by this study (cf. the section on magnetism below), all calculations concerning structural effects were carried out in the FM configuration, just to avoid the computational complexity of symmetry lowering in the AF case. We believe that the features of the equilibrium structure and its changes with pressure should not be affected by the type of magnetic configuration, owing to the small energy difference between the FM and AF cases. On the other hand, computations were performed with both the AE and PP basis sets.

The unit-cell volume was set to ten values ranging from -10 to $+8\%$ of the experimental result,[8] and the total energy was calculated keeping the c/a ratio and the z(Fe) and x(O) fractional coordinates fixed at their measured values. These three structural variables were relaxed for some of the points (-8, -4, 0, $+4$, $+8\%$) with the PP basis set, and their least-energy values turned out to vary linearly with the volume change. Therefore, with the AE basis set the relaxation was carried out for the -8 and $+4\%$ points only, interpolating linearly for the other values. In both cases, relaxation energy corrections vs volume were derived, finally obtaining numerical curves for $E(V)$, $c/a(V)$, $z_{Fe}(V)$, and $x_O(V)$. The whole procedure is described in more detail in previous work on $MgCO_3$ and α-Al_2O_3, which have the same space group.[22,6] The $E(V)$ curve was interpolated by the Murnaghan equation of state,[23,6] containing the zero-pressure energy (E_0), volume (V_0), elastic bulk modulus (K_0), and its pressure derivative (K_0') as fitting parameters. By differentiation, the pressure $p=-dE/dV=p(V)$ is obtained. Thus, all the above dependences of structural variables on volume were transformed into pressure dependences. The minimum of the Murnaghan curve $E(V)$ gives the equilibrium (zero-pressure) values of all such variables, which are reported in Table II and compared with the corresponding experimental values. The latter ones are taken from x-ray measurements at room temperature[8] and could not be extrapolated to $T=0$ K because of lacking thermal expansion data in the literature.

In all cases, a better agreement between calculated and measured data is observed for the AE with respect to PP results. This proves that the larger computational effort of the AE basis is definitely worthwhile, in order to simulate structural properties. As usual, with Hartree-Fock results for systems including fourth-row or heavier atoms, the least-energy unit-cell edges and volume are overestimated; this effect is larger for the *a* than *c* edge, resulting in a slight decrease of the c/a ratio with respect to its experimental value. The volume error ($+3.6\%$) is significantly worse than for the isostructural α-Al_2O_3 containing the light Al atoms (-0.2%),[6] but surprisingly performs better than for MnO ($+5.4\%$).[3] The most significant interatomic distances and angles (Fig. 1) are also reported in Table II, and will be particularly useful below for the discussion of magnetic properties. Here we need only remark that in the computed structure, the shortest Fe-O distance lengthens, but the longest does not, so as to reduce their difference with respect to experimental values.

The other parameters of the fitting to the Murnaghan equation of state also appear in Table II, except for the minimum energy E_0 (Table III). The experimental value of the bulk elastic modulus K_0 therein reported comes

TABLE II. Calculated (least-energy) and experimental equilibrium values (see the text for references) of hexagonal unit-cell edges (Å), volume per formula unit (Å^3), atomic fractional coordinates, selected interatomic distances (Å) and angles (deg), elastic bulk modulus (GPa), and its pressure derivative for α-Fe_2O_3. Linear compressibilities (TPa^{-1}) are reported, too. Percentage errors are indicated; PP and AE mean results obtained with pseudopotential and all-electron basis sets, respectively.

	PP	AE	exp.
a_0	5.144(+2.2%)	5.112(+1.5%)	5.035
c_0	13.893(+1.1%)	13.820(+0.5%)	13.747
c_0/a_0	2.701(−1.1%)	2.703(−1.0%)	2.730
V_0	53.06(+5.5%)	52.13(+3.6%)	50.30
x(O)	0.3003	0.3020	0.3056
z(Fe)	0.3539	0.3541	0.3553
Fe-O	2.005	1.988	1.945×3
	2.114	2.110	2.113×3
Fe1-Fe2	2.887	2.877	2.895
	3.444	3.421	3.361×3
	3.766	3.744	3.701×3
Fe1-O-Fe2	86.1	86.0	86.5
	118.4	118.8	119.6
	132.2	132.0	131.6×2
K_0	243(+6%)	261(+13%)	230
K_0'	3.3(−6%)	3.1(−11%)	3.5
$d(a/a_0)/dp$	−0.97	−0.90	−1.27
$d(c/c_0)/dp$	−1.37	−1.29	−1.61
$d(ca_0/ac_0)/dp$	−0.41	−0.40	−0.34

from a room-temperature x-ray diffraction (synchrotron radiation) static compression measurement up to 50 GPa,[24] and should be, thus, underestimated by about −3% with respect to the value extrapolated to the athermal limit.[6] Therefore, the real error of computed data should be accordingly reduced, so as to be similar, for the AE case, to the figure usually observed also for lighter substances.[6] A smaller error is observed with the PP basis set, which is, however, due to the larger computed unit-cell volume, producing a reduced elastic stiffness, with respect to the AE case. It should also be noticed that a more accurate K_0 experimental value would be given by knowledge of all elastic constants, but unfor-

TABLE III. Total energies per formula unit (hartree) for α-Fe_2O_3 (E_0) and for individual atoms, and binding energy E_B of α-Fe_2O_3. Hartree-Fock results and HF + electron correlation corrections[27] are reported for the AE basis set. Δ% is the percentage error with respect to the experimental binding energy of 0.9250 hartree.

	HF	HF + corr
E(Fe)	−1262.3679	−1263.5895
E(O)	−74.8012	−75.0672
$E_0(\alpha$-$Fe_2O_3)$	−2749.7835	−2753.1915
E_B	−0.6441	−0.8109
Δ%	−30.4	− 12.3

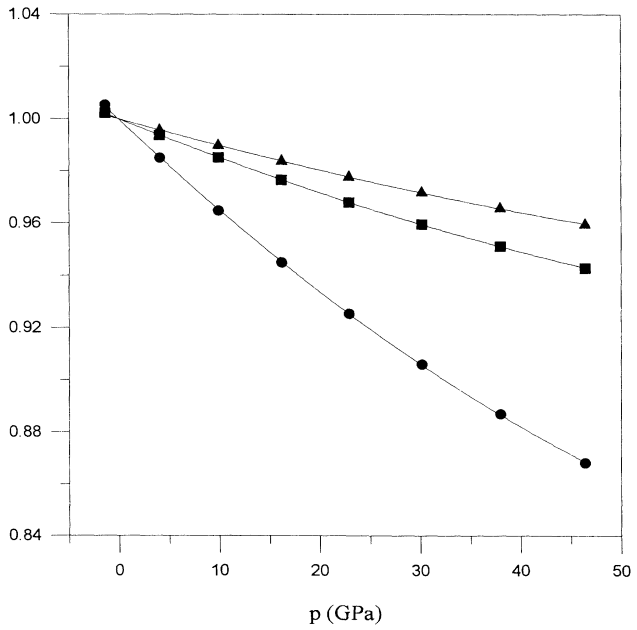

FIG. 2. Calculated dependence of the unit-cell constants of α-Fe_2O_3 divided by their equilibrium values on pressure. Triangles, squares, and circles indicate the a/a_0, c/c_0, and V/V_0 ratios, respectively.

tunately the C_{13} component was not measured;[25] the set of elastic components necessary to calculate the bulk modulus is incomplete. Values of K_0 obtained in older static compression studies[7,8] compare well with those reported in Table II.

The curves of V/V_0, a/a_0, and c/c_0 versus pressure are shown in Fig. 2. Least-squares linear approximations of the p dependences of a/a_0, c/c_0, and $(c/a)/(c_0/a_0)$ give the slopes reported in Table II, and are therein compared to values obtained from linear fits of the data of Ref. 8. The behavior of c/a is particularly interesting, because its pressure coefficient turns out to be three times larger than that of α-alumina. This reproduces closely what is observed experimentally in a much smaller pressure range, and shows that hematite is much more compressible along the threefold axis than the isostructural α-Al_2O_3. The computed compressibilities seem to be slightly smaller than the measured ones, for which the estimated error should be of the order of 10%.

BINDING ENERGY

The results of calculations performed to obtain the binding energy of α-Fe_2O_3 are summarized in Table III. Atomic energies of isolated Fe and O atoms were computed by using the same all-electron basis sets used in the crystal, but supplemented by two more diffuse shells, the exponents of which were optimized. In the case of Fe, 0.127 and 0.044 bohr^{-2} were obtained, and also the exponents of the 5*sp* and 4*d* shells were reoptimized to 0.552 and 0.392 bohr^{-2}, respectively. The binding energy E_B is obtained as the difference between the total crystal energy per formula unit E_0 (with optimized structural geometry) and the energies of the constituent isolated atoms. The experimental value of E_B was derived by an appropriate Born-Haber thermochemical cycle, according to the relationship

$$E_B(\text{expt}) = \Sigma_i [H^0_{a,i} + (H_i^{298} - H_i^0)] + \Delta H_f^{298} - (H^{298} - H^0) - E^0_{\text{vib}} \ .$$

The sum is extended to all chemical elements in the formula unit. The formation enthalpy ΔH_f^{298} of α-Fe_2O_3, sublimation (Fe) and dissociation (O_2) enthalpies $H^0_{a,i}$, and heating enthalpies $H_i^{298} - H_i^0$ for all three species were taken from Ref. 26. The zero-point vibrational energy of hematite E^0_{vib} was estimated by the Debye model, using an isotropic approximation for the mean acoustic wave velocity derived from the bulk modulus, which gave a Debye temperature of 911 K. A value of 0.9250 hartree was, thus, obtained for the experimental binding energy of α-Fe_2O_3.

As usual, the Hartree-Fock binding energy turns out to be underestimated by about 30%. The *a posteriori* correction of total energies based on an estimate of the correlation energy obtained by density-functional theory[27] leads to a considerable improvement. The error obtained (−12%) is comparable to that found for MnO and NiO (Ref. 19), but appears to be slightly larger with respect to results relative to systems with the same structures but containing lighter atoms.[6]

MAGNETIC PROPERTIES

The energy difference between the antiferromagnetic and the ferromagnetic configurations, ΔE(AF-FM), was computed for the experimental crystal structure of hematite (Table IV). Hartree-Fock results uncorrected and corrected for the correlation energy are reported. The relative stabilities of the two magnetic structures are reproduced rightly, and this should be considered as an important achievement of the method of calculation, because of the small energy value involved. Use of the pseudopotential rather than all-electron scheme to represent the Fe atom seems to overestimate somehow the ΔE(AF-FM) energy. Performing the correction for correlation energy enhances the stability of the antiferromagnetic structure significantly, with respect to the bare Hartree-Fock result. On the other hand, most of the stabilization effect of the AF configuration is related to the superexchange mechanism of antiferromagnetism,[1,28] according to which the net spin moments of Fe1 and Fe2 atoms are coupled in an antiparallel way through overlap of the corresponding electron distributions with that of the in-between O atom. Further, such a mechanism is most effective when the Fe1-O-Fe2 bond angle approaches 180°, and its energy contribution decreases as this angle shrinks.[1,28] In hematite, the O atom is surrounded by four Fe atoms, two of Fe1 and two of Fe2 type (Fig. 1). Out of the six Fe-O-Fe′ angles, four are of Fe1-O-Fe2 type. Three of these are wider, 120° and 132° (×2), with Fe1-Fe2 distances of 3.361 and 3.701 (×2) Å, respectively. The fourth one (86.5°) is much smaller, and thus, though corresponding to the shortest Fe1-Fe2 contact (2.900 Å, parallel to the threefold *c* axis), should give little contribution, if any, to superexchange interactions.

Therefore, from the point of view of superexchange, the structure of hematite is much more complicated than those usually considered (typically, the rocksalt case), where metal-oxygen-metal angles are either 90° or 180°; thus this appears ideally suited to a deeper investigation of the structural features of superexchange. This has been done by computing the value of ΔE(AF-FM) for strained unit-cell geometries, with the PP basis set in order to contain the cost of calculations. Either the edge *a* or *c* was changed, keeping all other parameters fixed at their experimental equilibrium values; the energy

TABLE IV. Energy difference per formula unit ΔE(AM-FM) (hartree) between the antiferromagnetic and ferromagnetic configurations of hematite, computed at the experimental crystal structure, for the PP and AE basis sets.

	HF	HF + corr
PP	−0.0027	−0.0034
AE	−0.0019	−0.0027

TABLE V. Energy difference per formula unit (hartree) between antiferromagnetic and ferromagnetic configurations of hematite, computed by changing either the a or c unit-cell edge or the c/a ratio (at constant volume), and corresponding interatomic distances (Å) and angles (deg) relevant for superexchange. The PP basis set is used.

a	HF	HF + corr	Fe-O		Fe1-O-Fe2		
5.034	−0.0027	−0.0034	1.944	2.114	131.6	119.7	86.5
5.334	−0.0008	−0.0011	2.038	2.181	130.9	119.0	83.2
5.634	+0.0002	+0.0002	2.134	2.251	130.3	118.3	80.1
6.034	+0.0008	+0.0011	2.262	2.346	129.6	117.6	76.3
c	HF	HF + corr	Fe-O		Fe1-O-Fe2		
13.75	−0.0027	−0.0034	1.944	2.114	131.6	119.7	86.5
15.75	−0.0016	−0.0021	2.000	2.263	133.4	121.5	94.3
18.75	−0.0006	−0.0009	2.095	2.504	136.0	124.4	104.1
20.75	−0.0000	+0.0001	2.165	2.673	137.8	126.4	109.7
c/a	HF	HF + corr	Fe-O		Fe1-O-Fe2		
3.502	−0.0042	−0.0054	1.895	2.220	135.0	123.3	100.6
3.085	−0.0036	−0.0045	1.914	2.157	133.2	121.3	93.4
2.731	−0.0027	−0.0034	1.944	2.114	131.6	119.7	86.5
2.430	−0.0017	−0.0021	1.981	2.087	130.3	118.3	79.8
2.172	−0.0010	−0.0011	2.024	2.075	129.2	117.2	73.6
1.948	−0.0003	−0.0002	2.072	2.075	128.3	116.3	67.7

difference results, together with interatomic distances and angles involved in superexchange, are reported in Table V. Of course expanding the unit cell tends to destabilize the antiferromagnetic with respect to ferromagnetic spin configuration, thus finally leading to a change of sign of ΔE(AF-FM). However, the effect is much stronger for the a than for the c expansion; to achieve the stability inversion requires that either of the two edges be lengthened by 10 or 50%, respectively.

This can be understood mainly by considering that an expansion of the a edge causes the Fe1-O-Fe2 angles relevant for superexchange to decrease, while the opposite occurs for the c lengthening. Thus, in the latter case the expansion of Fe-O bond lengths, leading to a weaker superexchange, is contrasted by the widening of bond angles, which favors superexchange. It is then clear that a larger expansion is necessary in the c than in the a case, in order to achieve the same effect on ΔE(AF-FM). A second reason is also related to the shorter (1.94 Å) Fe-O bonds having directions closer to the (001) plane, and longer (2.11 Å) Fe-O bonds closer to the [001] axis. Therefore, the expansion of a produces a comparatively larger increase of the shorter bond with respect to the same expansion of c, yielding a stronger effect on ΔE(AF-FM). This analysis is confirmed by considering the effect of changing the c/a ratio at constant unit-cell volume on the AF stabilization energy (Table V). The main effect is the angular distortion, which, as c/a decreases, narrows all Fe1-O-Fe2 angles weaking the superexchange and destabilizing the AF with respect to the FM configuration. The average Fe-O distance remains approximately constant, but the increase of the shorter bond length has again a negative effect on superexchange larger than the positive effect due to the decrease of the longer distance.

By considering the significant contribution of the correlation correction to the energy of antiferromagnetic stabilization (Table IV), it turns out that exchange (including superexchange) effects[29] are not exclusively responsible for the type of magnetic ordering observed in this compound; but, the electron correlation plays a not negligible role as well.

ELECTRONIC PROPERTIES

We refer in this section to electronic properties of hematite computed (AE basis set) for the antiferromagnetic experimental crystal-structure geometry. In this case, by definition, Fe1 atoms have a net excess of α (spin-up) or β (spin-down) electrons, and Fe2 atoms have α and β populations exactly exchanged with respect to Fe1; the α and β electron populations of O atoms are perfectly balanced. Results concerning the ferromagnetic structure would show only minor differences, referring mainly to a slight unbalance of the spin-up–spin-down electrons on oxygen.

In Table VI, the $\alpha+\beta$ Mulliken population data per orbital shell of Fe and O atoms is reported, together with net charges and total α-β values. The corresponding results obtained in previous work[3] on isoelectronic MnO are also shown for comparison; this is made possible by the use of electron basis sets designed very similarly in the two oxides, as discussed above. The Fe net charge of $2.62|e|$ appears to be slightly larger than that of $2.30|e|$ obtained[6] for Al in α-Al_2O_3. Also the bond overlap populations (0.012 against $0.098|e|$ for Fe-O and Al-O, re-

TABLE VI. Mulliken population data of electron-charge distribution in atomic-orbital shells ($\alpha+\beta$) and net atomic spins ($\alpha-\beta$) for Fe and O in α-Fe_2O_3 (AF, this work) and Mn and O in MnO (AF_2, Ref. 3), with all-electron basis sets.

	α-Fe_2O_3		MnO	
	Fe	O	Mn	O
1*s*	2.000	1.997	2.000	1.997
2*sp*	8.085	2.678	8.082	2.640
3*sp*	2.348	2.540	2.164	2.626
4*sp*	4.315	2.494	4.291	2.601
5*sp*	1.340		1.486	
3*d*	4.356	0.036	4.502	
4*d*	0.939		0.611	
d ($\alpha+\beta$)	5.295		5.113	
Total ($\alpha+\beta$)	23.382	9.745	23.136	9.864
z (net charge)	+2.618	−1.745	+0.864	−1.864
d ($\alpha-\beta$)	4.726	0.0		
Total ($\alpha-\beta$)	4.741	0.0	4.924	0.0
exp. magnetic moment (μ_B)	4.9[a]		4.79, 4.58[b]	

[a]See Ref. 30.
[b]See Ref. 3.

spectively) support a slightly more ionic character of bonding in α-Fe_2O_3 with respect to α-Al_2O_3. Most of the charge back transfer from O^{2-} to Fe^{3+} goes into the *d* orbitals (0.30|*e*|), giving a population of 5.01 spin-up and 0.29 spin-down electrons. This effect of partial spin pairing in the *d* shell, due to charge transfer, is stronger than for isoelectronic Mn^{2+} in MnO; in that case 0.11|*e*| are transferred, so that 5.02α and 0.10β electrons populate the *d* orbitals. The computed spin magnetic moment of $4.74\mu_B$ compares favorably with the experimental result[30] of $4.9\mu_B$. Here a slight underestimate of measured data is observed, while the deviation has the opposite sign for the magnetic moment of MnO.[3] By considering the detailed atomic-shell populations, the outer anionic and cationic shells appear to be more populated in MnO than in α-Fe_2O_3, showing a slight shrinkage of the electron cloud in hematite related to the higher nuclear charge of Fe^{3+} with respect to Mn^{2+}. It can be noticed that the Ms-$X\alpha$ calculations on the FeO_6^{9-} cluster showed a much more covalent Fe-O bonding, with Fe net charges of 1.30 (Ref. 17) and 1.83|*e*| (Ref. 16), and a larger charge transfer from O^{2-} to Fe^{3+} (0.75|*e*|, Ref. 16), with respect to the present results for periodic, crystalline α-Fe_2O_3.

In Fig. 3 the density of electronic states (DOS) of antiferromagnetic α-Fe_2O_3 is shown. By considering the projections over atomic contributions therein outlined, we can interpret the sequence of peaks appearing from low to high energy as follows. The first one is a 2*s*(O) nonbonding band, followed by a narrow band of mainly $3d^{\alpha}$(Fe1) [or $3d^{\beta}$(Fe2)] character, with some admixture with 2*p*(O) states and thus a limited Fe-O bonding nature. The upper valence band, lying just below the Fermi energy, is essentially of 2*p*(O) nonbonding type with a minor presence of $3d^{\beta}$(Fe1) [or $3d^{\alpha}$(Fe2)] states due to charge transfer from O^{2-} to Fe^{3+} (cf. the discussion of electron populations above). A conduction band of $3d^{\beta}$(Fe1) character, with a small contribution from 2*p*(O) levels giving it some Fe-O antibonding nature, is finally observed

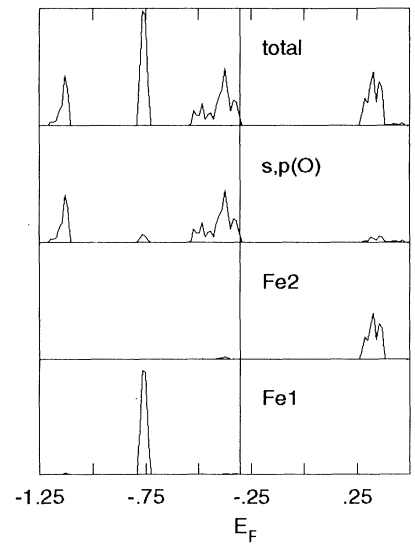

FIG. 3. DOS (density of electronic states, energy in hartrees) of antiferromagnetic α-Fe_2O_3 relative to spin-up electrons, with projections onto atomic-orbital contributions. The spin-down diagram would exchange the *d*(Fe1) and *d*(Fe2) projections, leaving the rest unvaried.

above E_F. Some important features should be stressed. First, the band gap is of *p-d* instead of *d-d* type: thus α-Fe_2O_3 is shown by Hartree-Fock calculations to be a charge transfer rather than Mott-Hubbard insulator, just as was the case for MnO and NiO.[3] This confirms the results of experimental photoemission spectroscopy on hematite, interpreted on the basis of configuration-interaction calculations on the FeO_6^{9-} cluster.[12] The photoelectron spectrum of α-Fe_2O_3 shows a three-peak structure extending 18 eV below the Fermi level, with maxima at approximately -3.1, -6.2, and -12.9 eV.[13] The first two peaks are assigned to $3d^5L$ photoemission final states, which result from L (O^{2-}ligand)$\rightarrow d$ (Fe^{3+} metal) charge transfer transforming the original metal d holes (d^4 states) into ligand p holes. The region in the lower energy range (-9 to -18 eV), including the third peak, is ascribed to $3d^4$ final states (d holes). Since $3d^nL$ instead of $3d^{n-1}$ final states are located near the Fermi level in the photoemission spectra, ferric oxide is classified as a charge transfer rather than Mott-Hubbard insulator.[31] There is a surprising agreement between this scheme and the Hartree-Fock density of states shown in Fig. 3, concerning not only qualitatively the relative positions of the $3d(Fe^{3+})$ and $2p(O)$ valence bands, but also the quantitative energy values of density maxima. This would indicate that in the present case the Koopman's theorem holds successfully, so that effects of relaxation of the electron configuration after the ionization process would play a minor role, at least to a first approximation. Further, contrary to arguments in favor of a $4s(Fe^{3+})$ nature of the lower conduction band,[12] inverse-photoemission spectra of hematite[15] have shown that the empty states just above E_F have a $3d(Fe^{3+})$ character, thus fully confirming the DOS of Fig. 3 also above the Fermi level.

Coming now to details, and comparing with the DOS's of rocksalt type MnO and NiO, we observe that (i) the $3d^{\alpha}(Fe^{3+})$ band is very narrow (less than 3 eV) with t_{2g} and e_g states practically superposed, so as to give a nearly vanishing crystal-field splitting, and (ii) the $3d^{\alpha}(Fe^{3+})$ and $2p(O^{2-})$ bands are separated by an energy gap. On the other hand, the DOS's of MnO and NiO show a wide $3d$ band (over 8 eV) overlapping largely with the $2p(O)$ one, and including separated peaks contributed by t_{2g} and e_g states. These features would support a more localized character of the metal d states in hematite than in MnO and NiO, probably because of the different characters of the corundum and rocksalt structures: in the former, the metal coordination octahedra are much less condensed in space than in the latter. Further, although all three oxides are charge-transfer insulators, α-Fe_2O_3 shows this character more strongly, while MnO and NiO seem a bit more inclined towards the Mott-Hubbard régime. It can be finally remarked that the charge transfer from $2p(O^{2-})$ to $3d^{\beta}(Fe^{3+})$ states, estimated as $0.29|e|$ by the Mulliken population results, lies between the values of 0.21 calculated by the CI cluster model[12] and that of $0.4|e|$ suggested by a Mössbauer study of hyperfine fields in $Fe_{2-x}Rh_xO_3$.[32] Such a charge transfer is proved to give rise to a partial Fe-O σ bonding character of the upper valence band by the above analysis of the DOS, and thus to be responsible of the (small) covalency observed in α-Fe_2O_3.

The electron-charge difference between crystal and ionic superposition is shown for the plane (010) in Fig. 4(a).

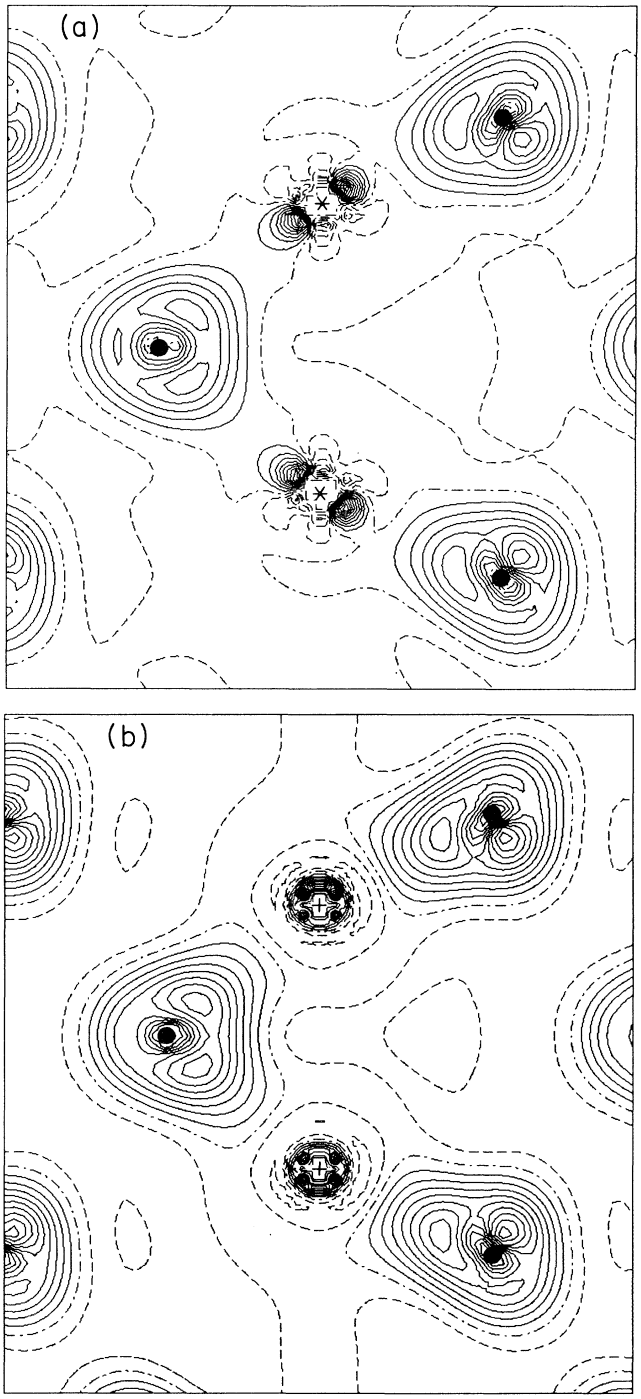

FIG. 4. Difference (crystal minus ionic superposition) charge-density maps on the (010) hexagonal plane for α-Fe_2O_3 (a) and α-Al_2O_3 (b, from data of Ref. 6). Three O (dots) and two Fe (stars) or Al (crosses) atoms are shown. Isodensity curves are separated by $0.04e$ Å^{-3}. Continuous, dashed-dotted, and dashed lines indicate positive, zero, and negative values, respectively.

No metallic bonding density appears between adjacent Fe atoms along the [001] direction, contrary to what was reported in some x-ray diffraction studies.[33,34] Such a feature is not reproduced even by previous theoretical work on hematite; in our opinion, the interpretations given to these experimental results[34] should be taken cautiously, because the same authors claim to have observed a similar metal-metal bond also in α-Al_2O_3,[35] and this is in contrast with other careful experimental studies[36,37] and also with physicochemical intuition. Thus, the Al-Al bonding in corundum and Fe-Fe in hematite may be artifacts related to an inadequate account of extinction effects and/or absolute scale factor in the diffraction studies. An interesting aspect should be noticed in Fig. 4(a): the two lobes of highly concentrated charge difference around each Fe^{3+} ion, pointing towards its two neighboring oxygens. These peaks account for the charge transfer $2p(O^{2-}) \rightarrow 3d^{\beta}(Fe^{3+})$, and their orientation corresponds to the small Fe-O σ-type bonding due to d(Fe)/p(O) band superposition as apparent from the DOS results (Fig. 3). In Fig. 4(b), the corresponding picture of electron-density difference for α-Al_2O_3 (Ref. 6) is shown, and the spherical distribution surrounding Al^{3+} ions contrasts sharply with that of Fe^{3+}. Figure 5(a) and 5(b) show the spin densities (α-β) of hematite for the antiferromagnetic and ferromagnetic structures, respectively. In the AF case, the symmetrical exchange of α and β 3d-type electrons in the Fe1 and Fe2 atoms appears clearly. In the FM structure, on the other hand, Fe1 and Fe2 have the same spins but a net spin polarization density is induced on the oxygen atoms, corresponding to a population of 0.11 α-β electrons derived from the Mulliken analysis.

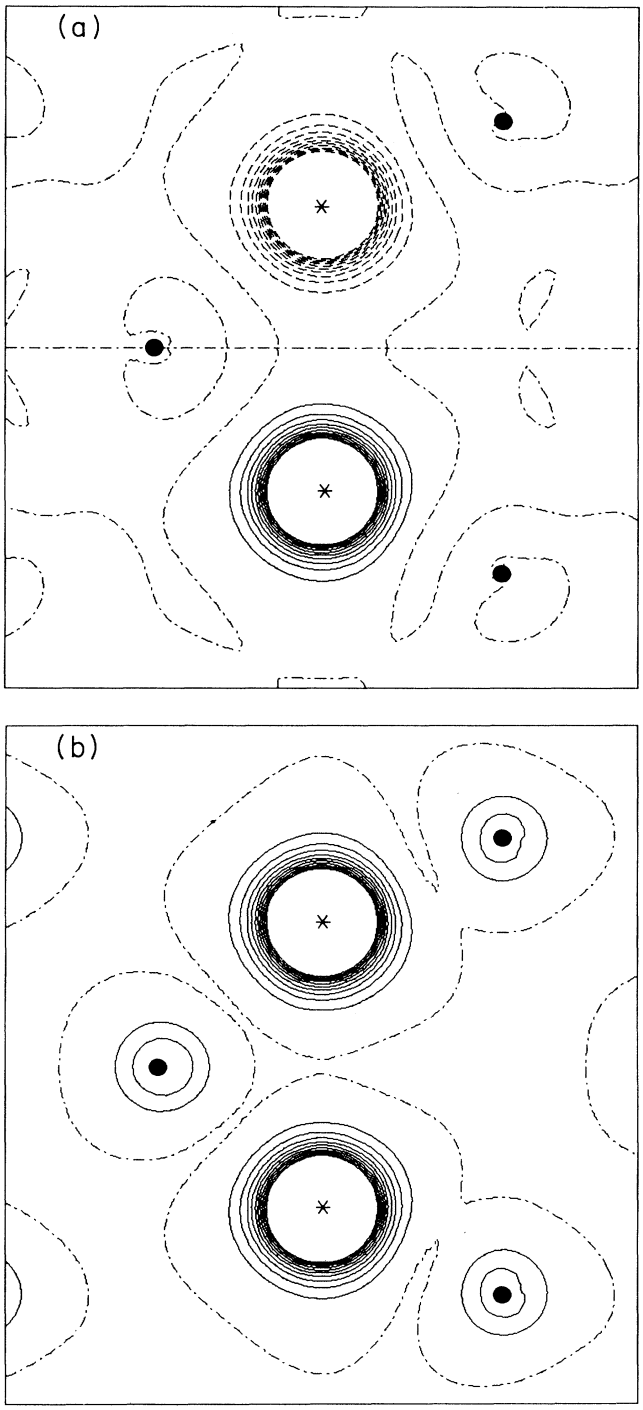

FIG. 5. Difference spin-density (spin-up minus spin-down) maps on the (010) hexagonal plane for antiferromagnetic (a) and ferromagnetic (b) α-Fe_2O_3. Isodensity curves are separated by 0.20e Å^{-3}. Continuous, dashed-dotted, and dashed lines indicate positive, zero, and negative values, respectively.

CONCLUSIONS

The electronic, magnetic, and structural behavior of corundumlike rhombohedral α-Fe_2O_3 has been simulated correctly by *ab initio* periodic unrestricted Hartree-Fock calculations. This includes its nature of charge-transfer insulator due to a p-d band gap, and the overall features of the valence band in the density of states, compared to photoelectron spectra. A large charge transfer from O^{2-} to the $3d^5$ metal ion states, leading to a smaller magnetic momentum, is observed with respect to the similar case of MnO. By comparing the relative energies of the antiferromagnetic and ferromagnetic structures, the former turns out to be more stable, consistently with experiment. Further, it has been possible to study in detail the effects of structural deformations on the relative stabilities of the two magnetic structures, throwing light onto the importance of bond angles in superexchange, and finding in some instances a stabilization of the ferromagnetic configuration. Finally, the evolution of the crystal structure with pressure has been determined up to nearly 50 GPa, deriving the compressibilities of unit-cell edges and of bond lengths. In particular, the c/a ratio proves to decrease with pressure much more rapidly than calculated previously in the case of isostructural α-Al_2O_3.

ACKNOWLEDGMENTS

We thank V. R. Saunders and M. D. Towler for providing the basis set of the isolated Fe^{3+} ion. The work was supported by the Human Capital and Mobility Programme of the European Union under Contract No. CHRX-CT93-0155, and by the Ministero Università e Ricerca Scientifica e Tecnologica, Roma.

[1]P. A. Cox, *The Transition Metal Oxides* (Oxford University Press, Oxford, 1992).
[2]W. C. Mackrodt, N. M. Harrison, V. R. Saunders, N. L. Allan, M. D. Towler, E. Aprà, and R. Dovesi, Philos. Mag. A **68**, 653 (1993).
[3]M. D. Towler, N. L. Allan, N. H. Harrison, V. R. Saunders, W. C. Mackrodt, and E. Aprà, Phys. Rev. B **50**, 5041 (1994).
[4]P. I. Sorantin and K. Schwarz, Inorg. Chem. **31**, 567 (1992).
[5]P. Dufek, K. Schwarz, and P. Blaha, Phys. Rev. B **48**, 12 672 (1993).
[6]M. Catti, G. Valerio, R. Dovesi, and M. Causà, Phys. Rev. B **49**, 14 179 (1994).
[7]Y. Sato and S. Akimoto, J. Appl. Phys. **50**, 5285 (1979).
[8]L. W. Finger and R. M. Hazen, J. Appl. Phys. **51**, 5362 (1980).
[9]C. N. R. Rao and J. Gopalakrishnan, *New Directions in Solid State Chemistry* (Cambridge University Press, Cambridge, England, 1986).
[10]T. G. Worlton, R. B. Bennion, and R. M. Brugger, Phys. Lett. **24A**, 653 (1967).
[11]A. Tasaki and S. Iida, J. Phys. Soc. Jpn. **18**, 1148 (1963).
[12]A. Fujimori, M. Saeki, N. Kimizuka, M. Taniguchi, and S. Suga, Phys. Rev. B **34**, 7318 (1986).
[13]R. J. Lad and V. E. Henrich, Phys. Rev. B **39**, 13 478 (1989).
[14]G. Draeger, W. Czolbe, and J. A. Leiro, Phys. Rev. B **45**, 8283 (1992).
[15]F. Ciccacci, L. Braicovich, E. Puppin, and E. Vescovo, Phys. Rev. B **44**, 10 444 (1991).
[16]S. Nagel, J. Phys. Chem. Solids **46**, 905 (1985).
[17]D. M. Sherman, Phys. Chem. Miner. **12**, 161 (1985).
[18]R. Dovesi, V. R. Saunders, and C. Roetti, *CRYSTAL92.* User's Manual, Gruppo di Chimica Teorica (Università di Torino, Torino, 1992).
[19]E. Aprà, Ph.D. thesis, University of Torino, 1993.
[20]W. H. Hehre, L. Random, P. R. Schleyer, and J. A. Pople, *Ab Initio Molecular Orbital Theory* (Wiley, New York, 1986).
[21]P. Durand and J. C. Barthélat, Theor. Chim. Acta **38**, 283 (1975).
[22]M. Catti, A. Pavese, R. Dovesi, and V. R. Saunders, Phys. Rev. B **47**, 9189 (1993).
[23]F. D. Murnaghan, Proc. Natl. Acad. Sci. U.S.A. **30**, 244 (1944).
[24]J. Staun Olsen, C. S. G. Cousins, L. Gerward, H. Jhans, and B. J. Sheldon, Phys. Scr. **43**, 327 (1991).
[25]R. C. Liebermann and S. K. Banerjee, J. Geophys. Res. **76**, 2735 (1971).
[26]*Handbook of Chemistry and Physics,* edited by R. C. Weast (Chemical Rubber, Boca Raton, 1987).
[27]J. P. Perdew, J. A. Chevary, S. H. Vosko, K. A. Jackson, M. R. Pederson, D. J. Singh, and C. Fiolhais, Phys. Rev. B **46**, 6671 (1992).
[28]L. J. de Jongh and R. Block, Physica B+C **79B**, 568 (1975).
[29]J. H. van Vleck, J. Chem. Phys. **9**, 85 (1941).
[30]E. Krén, P. Szabó, and G. Konczos, Phys. Lett. **19**, 103 (1965).
[31]J. Zaanen, G. A. Sawatzky, and J. W. Allen, Phys. Rev. Lett. **55**, 418 (1985).
[32]J. M. D. Coey and G. A. Sawatzky, J. Phys. C **4**, 2386 (1971).
[33]V. G. Tsirel'son, M. Yu. Antipin, V. A. Strel'tsov, R. P. Ozerov, and Yu. T. Struchkov, Dokl. Akad. Nauk SSSR **298**, 1137 (1988) [Sov. Phys. Dokl. **33**, 89 (1988)].
[34]E. N. Maslen, V. A. Strel'tsov, N. R. Streltsova, and N. Ishizawa, Acta Crystallogr. Sec. B **50**, 435 (1994).
[35]E. N. Maslen, V. A. Streltsov, N. R. Streltsova, N. Ishizawa, and Y. Satow, Acta Crystallogr. Sec. B **49**, 973 (1993).
[36]A. S. Brown, M. A. Spackman, and R. J. Hill, Acta Crystallogr. Sec. A **49**, 513 (1993).
[37]A. Kirfel and E. Eichhorn, Acta Crystallogr. Sec. A **46**, 271 (1990).